Supporting Information for

Enhanced cycling stability of boron-doped lithium-rich layered oxide cathode materials by suppressing transition metal migration

Zhenhe Sun,[a] Lingqun Xu,[a] Caiqiao Dong,[a] Hongtao Zhang,[a,b] Mingtao Zhang,[a] Yiyang Liu,[a] Ying Zhou,[a] Yu Han,[a] Yongsheng Chen*[a,b]

a. The Centre of Nanoscale Science and Technology and Key Laboratory of Functional Polymer Materials, Nankai University, Tianjin, 300071, China.

b. The National Institute for Advanced Materials, Nankai University, Tianjin 300071, China.

E-mail: yschen99@nankai.edu.cn

Table S1. The refinement of LLO and LLO@LBO.

(a) The refinement of XRD results for LLO in Figure 1.

Crystal system	Hexagonal				R_p=4.04%
Space group	R-3m				R_{wp}=5.01%
Atom	Site	x	y	z	Occupancy
Li_1	3a	0	0	0	0.8661
Ni_1	3a	0	0	0	0.1297
Mn	3b	0	0	0.5000	0.3400
Co	3b	0	0	0.5000	0.3330
O	6c	0	0	0.2433	1.0000
Li_2	3b	0	0	0.5000	0.0150
Ni_2	3b	0	0	0.5000	0.3150

(b) The refinement of XRD results for LLO@LBO in Figure 1.

Crystal system	Hexagonal				R_p=1.95%
Space group	R-3m				R_{wp}=2.51%
Atom	Site	x	y	z	Occupancy
Li_1	3a	0	0	0	0.8489
Ni_1	3a	0	0	0	0.1511
Mn	3b	0	0	0.5000	0.3400
Co	3b	0	0	0.5000	0.3330
O	6c	0	0	0.2430	1.0000
Li_2	3b	0	0	0.5000	0.0150
Ni_2	3b	0	0	0.5000	0.3150

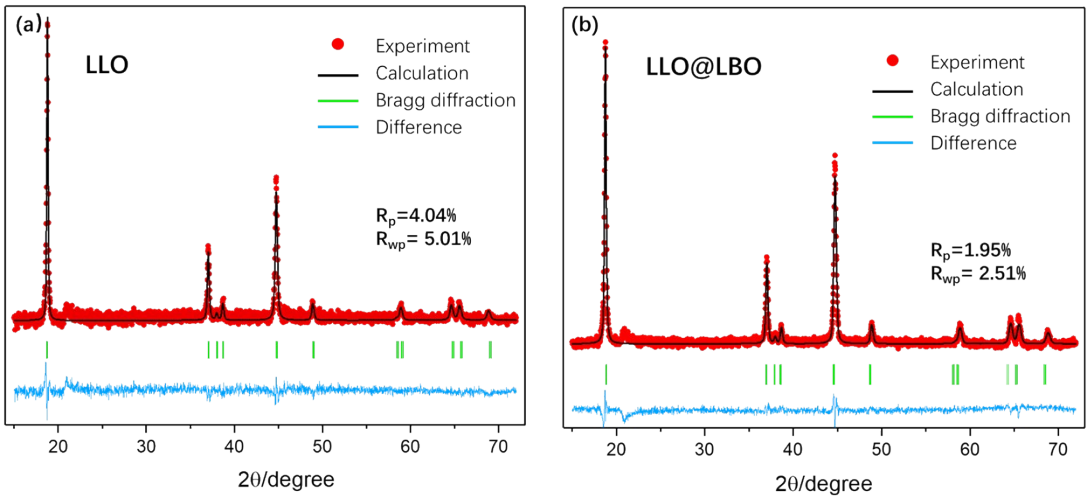

Figure S1. Refinement results of LLO@LBO and bare LLO.

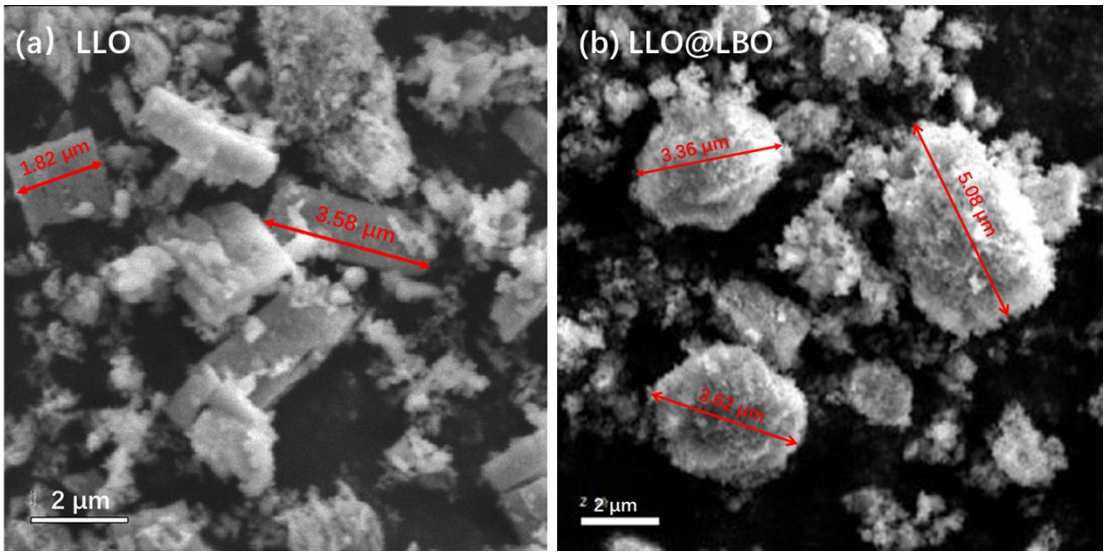

Figure S2. The SEM images of LLO and LLO@LBO.

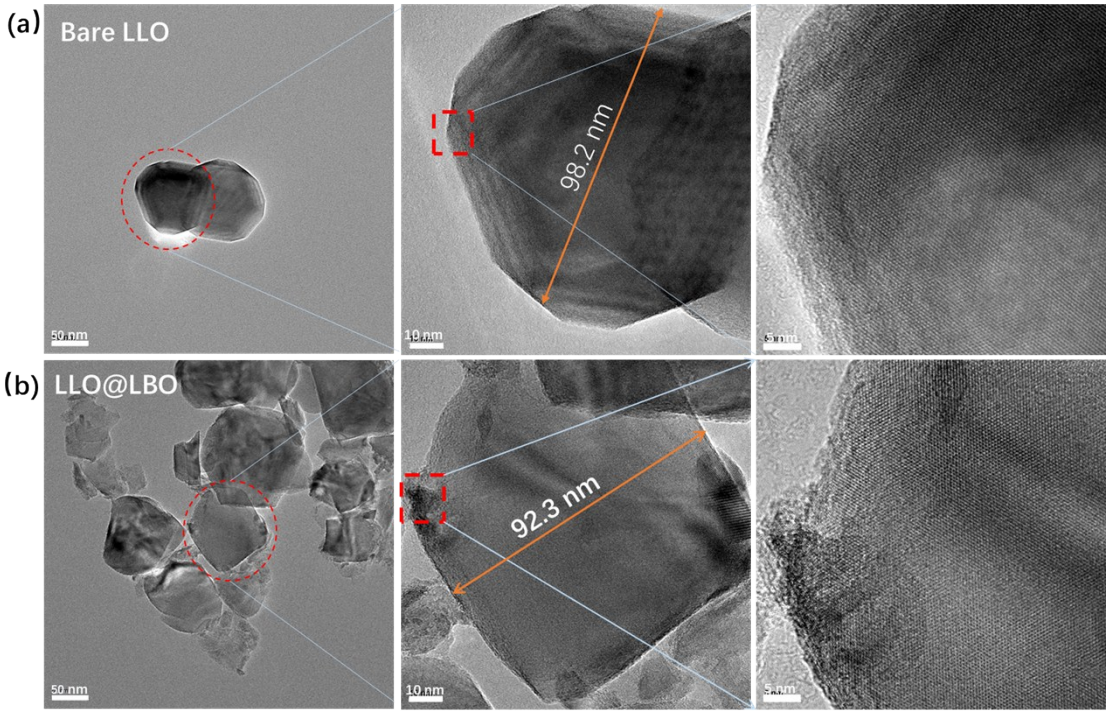

Figure S3. HRTEM images of (a) bare LLO and (b) LLO@LBO.

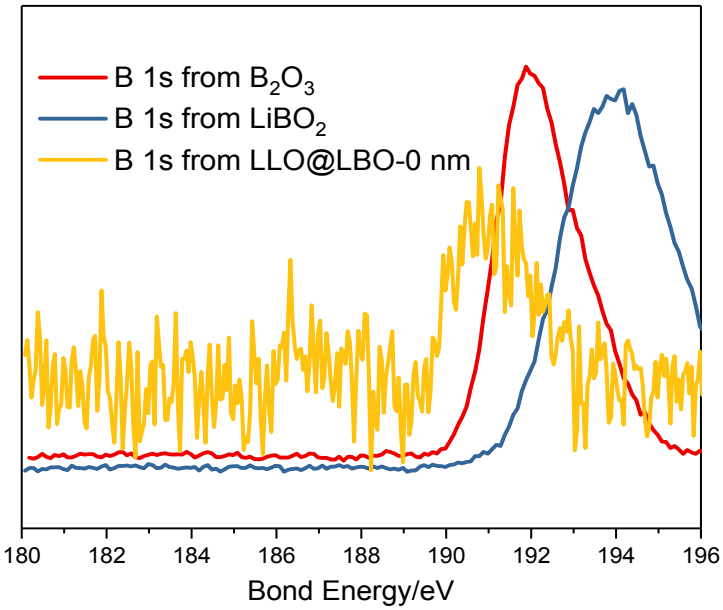

Figure S4. The XPS spectrums of B 1s in LLO@LBO (0 nm), $LiBO_2$ and B_2O_3.

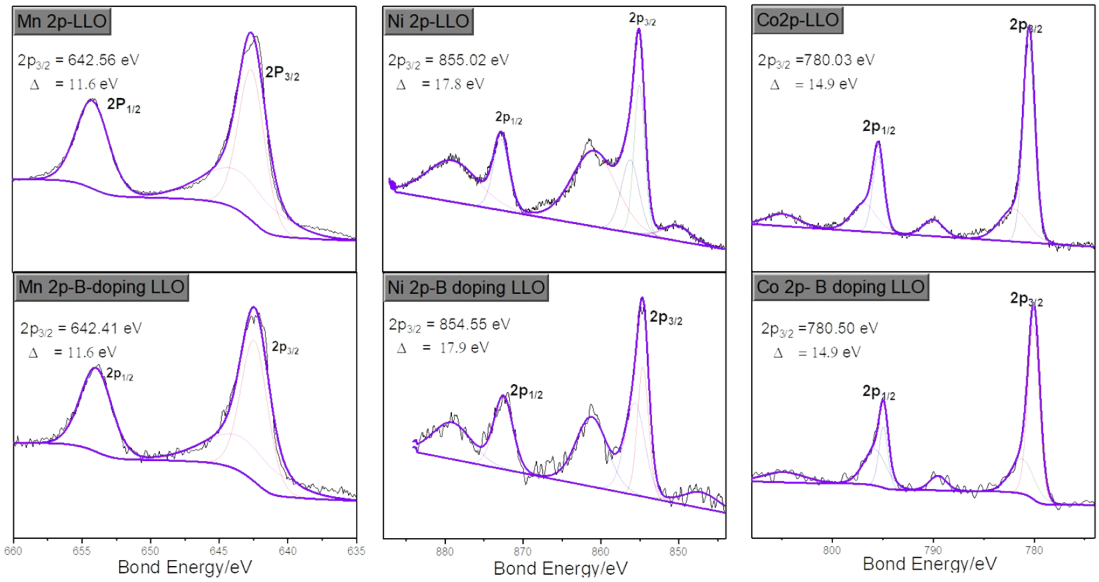

Figure S5. The XPS spectrum of Ni 2p, Co 2p, and Mn 2p at surface with and without boron doping.

The XPS spectrum of Ni 2p, Co 2p, and Mn 2p at surface with and without boron doping are compared in Figure S1. The XPS plots of Ni, Co and Mn is well accord with the previous work.[1, 2] Furthermore, the position of each peak shows no visible change before and after boron doping. It demonstrate that the boron doping hardly affects the chemical valence of transition metal.

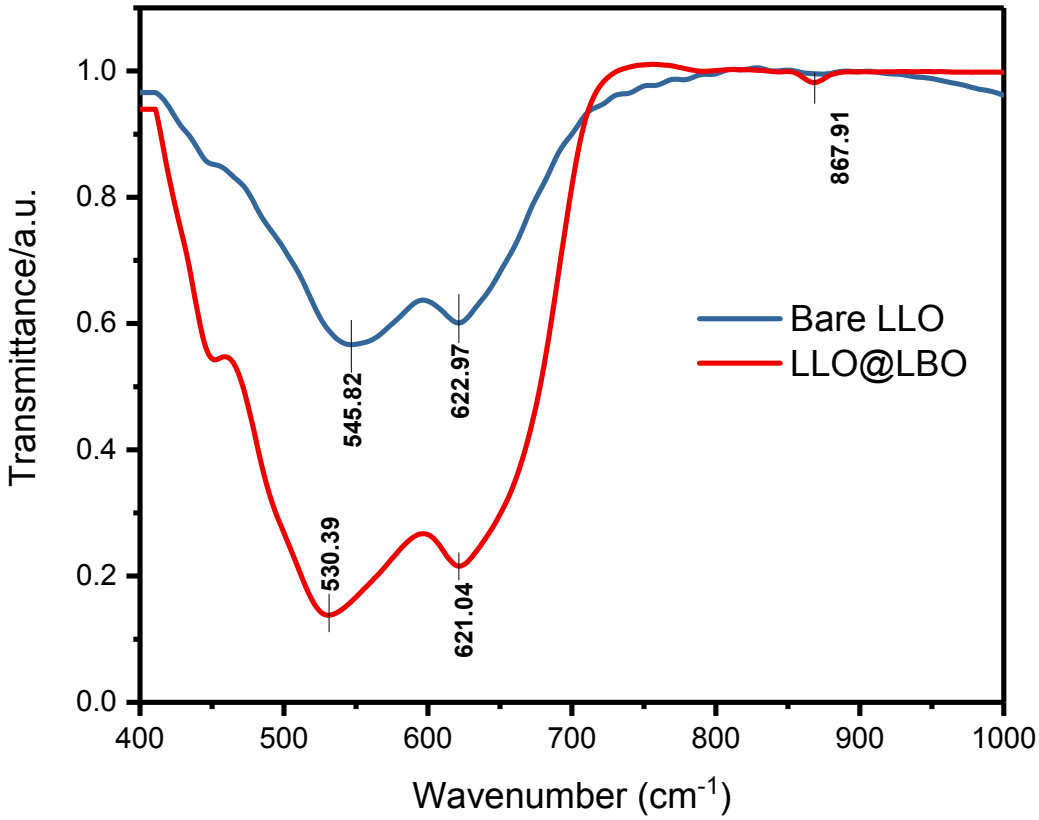

Figure S6. The FT-IR of LLO@LBO and bare LLO.

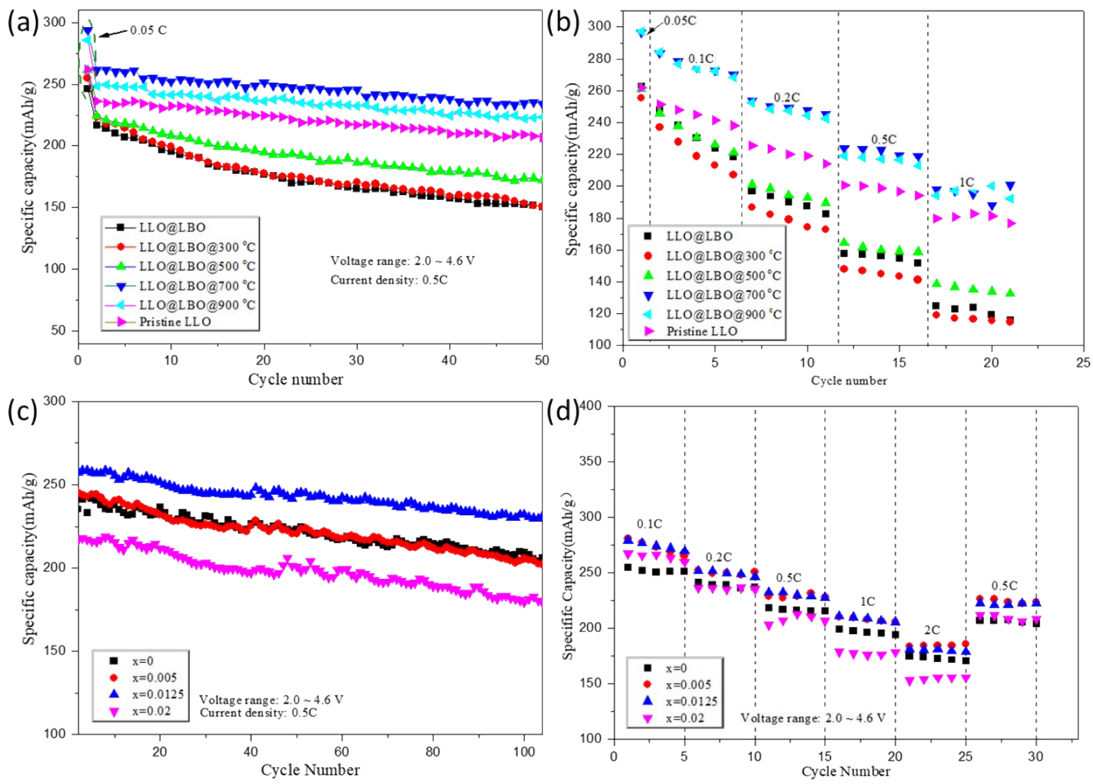

Figure S7. (a) The cycle ability and (b) rate performance of LLO@LBO at different reaction temperature (300, 500, 700, and 900 ℃). (c) The cycle ability and (b) rate performance of $Li_{1.2}Ni_{0.13}Co_{0.13}Mn_{0.54}B_xO_2$ with x= 0, 0.005, 0.0125 and 0.02.

We optimized the reaction temperature and boron content for the doping process. the results shows that the LLO@LBO with x=0.0125 and a reaction temperature of 700 ℃ shows the best electrochemical performance. At lower temperature, boron atoms cannot be introduced into the lattice of LLO while higher temperature induce the structural damage. For boron content, excessive boron atoms also increase the inactive components and inhabit the lithium ion (TM layer) migration from TM layers to lithium layers, which causes the declined capacity performance

Table S2. The key information for multivalent ion doping of LLOs.

Doping ions	Mass percent	Initial CE	Reversible Capacity	Cycle retention	Reference
B	0.16%	90.77	293.9	89.6(100)	Our work
Mo	2.28%	77.2	270.6	88.7(100)	[3]
Zr	8.62%	67.7	210	78(100)	[4]
Nb	2.17%	82	281.3	83(100)	[5]
La	3.26%	70.02	263.1	93.9(100))	[6]
Gd	3.69%	80.1	273.6	90.9(100)	[7]
Sb	3.85%	87.8	272.8	86.9(100)	[8]
Al	1.58%	75	231.7	98(30)	[9]
Sn	1.39%	76.5	268.9	75.2(100)	[10]
Rb	3.0%	74.0	255	92.78(100)	[11]
Ga	1.6%	77.43	259.8	88.2(100)	[12]
Te	7.48%	88.2	271.6	84.3(100)	[13]
Ti	2.2%	62.94	187.8	99.4(10)	[14]
Se	12.9%	77	265	95(100)	[15]
Y	3.13%	77.6	235.5	92.7(50)	[16]
Fe	1.96%	83.4	261.6	90.9(80)	[17]
Ru	1.18%	76	277	81(50)	[18]

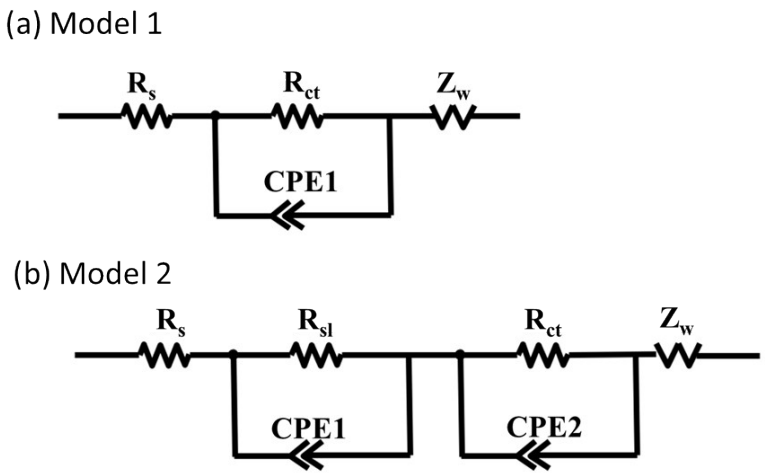

Figure S8. The equivalent circuits used for the fitting of Nyquist plots.

The fitting of the Nyquist plots of LLO and LLO@LBO electrode before cycling used the Model 1. That of cycled LLO@LBO electrode also adopted Model 1 as the fitting model. However, the Nyquist plots of cycled LLO electrode is simulated using the Model 2 due to its intrinsic difference from others.

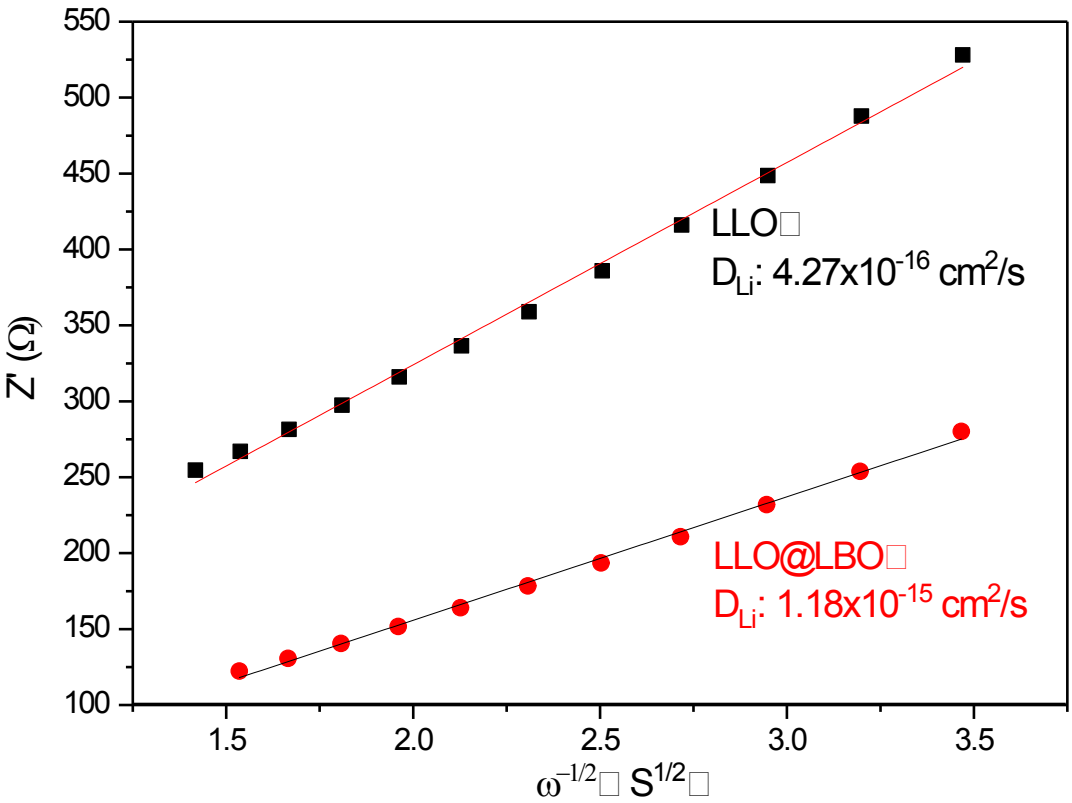

Figure S9. The plot of Z′ vs. $\omega^{-1/2}$ for LLO@LBO and bare LLO.

Table S3. The simulated results of Nyquist plots for LLO and LLO@LBO electrodes at discharge state of 2.0 V.

		R_s (Ω)	R_{sl} (Ω)	R_{ct} (Ω)
LLO	Fresh	2.186	N/A	79.55
	100 cycles	3.243	119.4	209.44
LLO@LBO	Fresh	2.865	N/A	56.54
	100 cycles	3.339	N/A	131.6

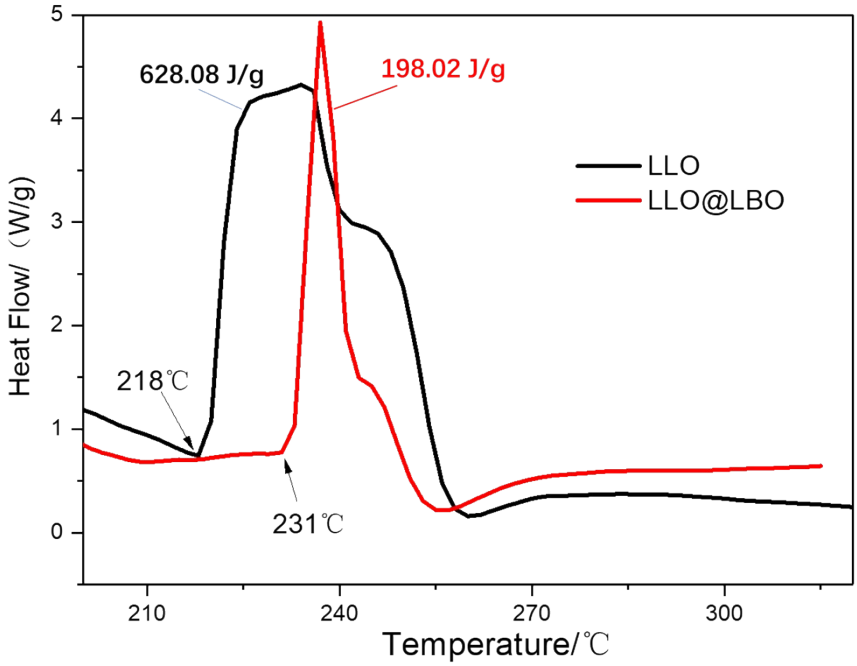

Figure S10. The DSC profiles of LLO@LBO and LLO charged at 4.6 V and kept for 10 h at constant voltage , at a scanning rate of 10 ℃ min^{-1}.

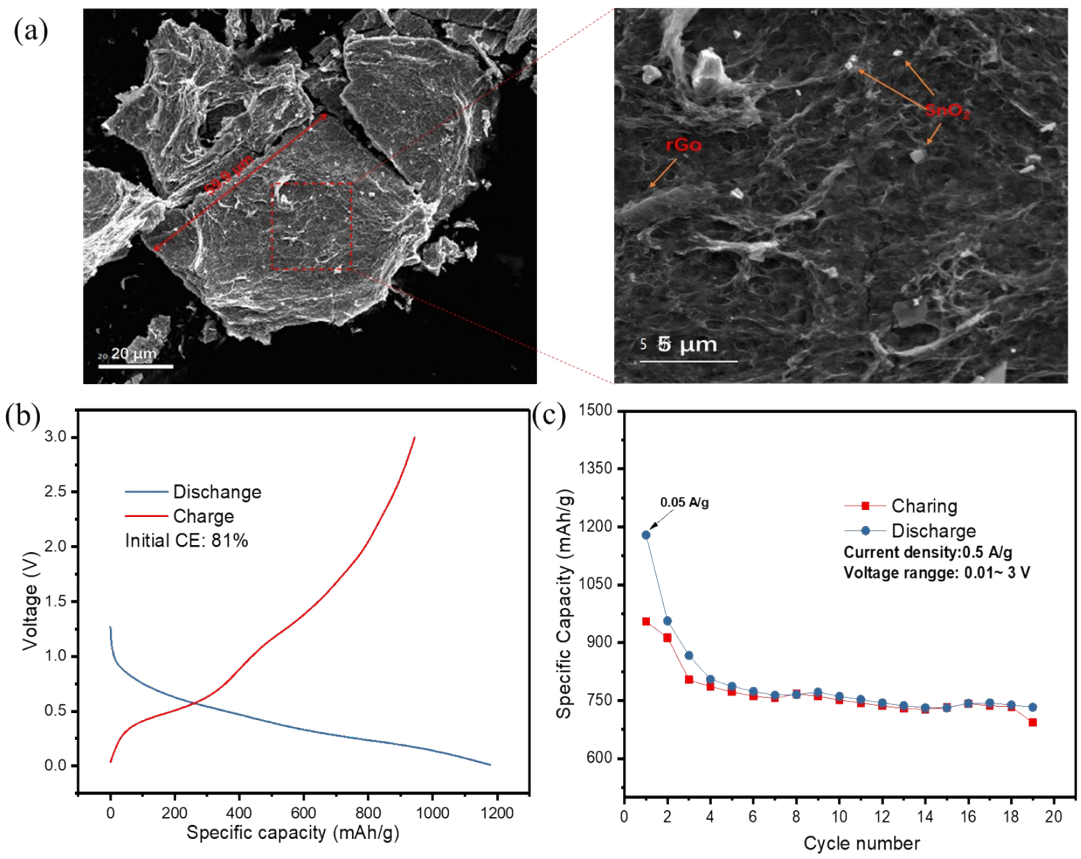

Figure S11. (a) The SEM image of SnO_2@rGO anode materials and its enlarged image, (b) the discharge/discharge curve of SnO_2@rGO at initial cycle and (c) the cycle performance of SnO_2@rGO anode materials.

Reference

1. G. Assat, D. Foix, C. Delacourt, A. Iadecola, R. Dedryvère and J.-M. Tarascon, *Nature Communications*, 2017, **8**, 2219.
2. N. H. Vu, J. C. Im, S. Unithrattil and W. B. Im, *Journal of Materials Chemistry A*, 2018, DOI: 10.1039/c7ta09118d.
3. Y. Lu, S. Shi, F. Yang, T. Zhang, H. Niu and T. Wang, *Journal of Alloys and Compounds*, 2018, **767**, 23-33.
4. P. P. Dahiya, C. Ghanty, K. Sahoo, S. Basu and S. B. Majumder, *Journal of the Electrochemical Society*, 2018, **165**, A3114-A3124.
5. X. Hu, H. Guo, W. Peng, Z. Wang, X. Li and Q. Hu, *Journal of Electroanalytical Chemistry*, 2018, **822**, 57-65.
6. M. Li, Y. Zhou, X. Wu, L. Duan, C. Zhang, F. Zhang and D. He, *Electrochimica Acta*, 2018, **275**, 18-24.
7. Z. Shen, D. Li, Y. Tang and C. Li, *Journal of Materials Science-Materials in Electronics*, 2018, **29**, 9717-9727.
8. R. Yu, Z. Zhang, S. Jamil, J. Chen, X. Zhang, X. Wang, Z. Yang, H. Shu and X. Yang, *Acs Applied Materials & Interfaces*, 2018, **10**, 16561-16571.
9. M. Luo, R. Zhang, Y. Gong, M. Wang, Y. Chen, M. Chu and L. Chen, *Ionics*, 2018, **24**, 967-976.
10. L. Zhou, J. Liu, L. Huang, N. Jiang, Q. Zheng and D. Lin, *Journal of Solid State Electrochemistry*, 2017, **21**, 3467-3477.
11. N. Li, Y.-S. He, X. Wang, W. Zhang, Z.-F. Ma and D. Zhang, *Electrochimica Acta*, 2017, **231**, 363-370.
12. T. Yu, J. Li, G. Xu, J. Li, F. Ding and F. Kang, *Solid State Ionics*, 2017, **301**, 64-71.
13. J. Meng, Z. Wang, L. Xu, H. Xu, S. Zhang and Q. Yan, *Journal of the Electrochemical Society*, 2017, **164**, A2594-A2602.
14. Y. Kou, E. Han, L. Zhu, L. Liu and Z. a. Zhang, *Solid State Ionics*, 2016, **296**, 154-157.
15. Q. Ma, R. Li, R. Zheng, Y. Liu, H. Huo and C. Dai, *Journal of Power Sources*, 2016, **331**, 112-121.
16. L. Sun, X. Yi, X. Ren, P. Zhang and J. Liu, *Journal of the Electrochemical Society*, 2016, **163**, A766-A772.
17. X. Liu, T. Huang and A. Yu, *Electrochimica Acta*, 2014, **133**, 555-563.
18. B. Song, M. O. Lai and L. Lu, *Electrochimica Acta*, 2012, **80**, 187-195.